



# Sustainable Lubrication/Cooling Systems for Efficient Turning Operations of $\gamma$ -TiAl Parts from the Aeronautic Industry

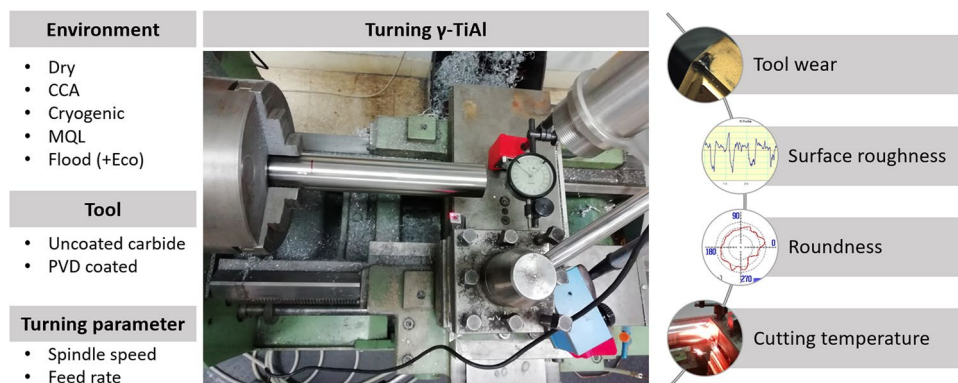
Elisabet Benedicto<sup>1,2,4</sup> · Eva María Rubio<sup>1</sup> · Laurent Aubouy<sup>2</sup> · María Ana Sáenz-Nuño<sup>3</sup>

Received: 2 September 2021 / Revised: 3 February 2022 / Accepted: 20 March 2022  
© The Author(s) 2022

## Abstract

This paper presents the study of the finishing, repair, and maintenance turning operations of gamma titanium aluminide ( $\gamma$ -TiAl) parts from the aeronautic industry, with the aim to evaluate different sustainable lubrication/cooling environments, including a newly developed synthetic ester water-based metalworking fluid (EcoMWF) to replace mineral-based MWF (MWF). The systems considered in this work are dry, cold-compressed air, minimum quantity lubrication (MQL), cryogenic, and flood on turning of a new and relatively low explored titanium alloy,  $\gamma$ -TiAl. Therefore, the influence of machining parameters and insert type on tool wear, surface roughness, roundness, and cutting temperature have been investigated for each environment. Results detailed in this study showed a significant influence of the lubrication/cooling systems on the machinability of  $\gamma$ -TiAl. The study also revealed that the sustainability of turning  $\gamma$ -TiAl could be improved under the cryogenic system and the new EcoMWF, keeping the same machining performance as common mineral-based MWF.

## Graphical abstract



**Keywords** Metalworking fluid ·  $\gamma$ -TiAl · Lubrication/cooling systems · Environmentally sustainable manufacturing · Turning operations · Aeronautic industry

## 1 Introduction

Gamma titanium aluminide ( $\gamma$ -TiAl), due to its excellent characteristics such as high elevated temperature strength and good oxidation resistance, has advanced applications in the automotive, aeronautic, and aerospace industries. The

difference in the working temperature could be 50% higher compared to other titanium alloys used, such as Ti6Al4V [1]. Moreover, titanium aluminides have become an alternative to replace heavy materials such as nickel-based superalloy to allow mass saving [2], and during the last years, several industries are introducing and qualifying this new alloy to produce their components [3]. Nevertheless, this new light-weight alloy is considered a difficult-to-machine material because of its low machinability rating [4]. The machining

✉ Elisabet Benedicto  
ebenedict6@alumno.uned.es

Extended author information available on the last page of the article



are related to the machining of  $\gamma$ -TiAl. Cold-compressed air (CCA) has a high cooling ability compared to other lubricating systems, and its flow helps break the chips, remove them from the cutting zone, and collect them in dry form. However, they do not have any lubricating capacity [18]. Therefore, CCA is commonly applied along with MQL in the form of spray or mist.

For difficult-to-machine materials, such as Ti6Al4V, cryogenic cooling has proved to be a successful alternative to MWF, thanks to the low temperature of the medium [19]. Liquid nitrogen ( $\text{LN}_2$ ) at  $-196^\circ\text{C}$  or liquid carbon dioxide ( $\text{CO}_2$ ) at  $-78^\circ\text{C}$  applied in the cutting zone, absorb the heat generated during cutting, and evaporates, providing no pollutant residue on the workpiece, chips, and machine tool. Moreover, it is considered a clean and environmentally friendly lubrication/cooling system with lubrication capacity by forming a gas layer between interfaces and providing significant benefits such as chip breakability, increased tool life, and surface quality improvement [20].

Regarding EcoMWF, vegetable oils and synthetic esters are considered potential alternatives to replace mineral oil-based fluids due to their high biodegradability, low toxicity, and high performance [21]. For turning titanium alloys, the use of water-based MWF is preferred due to its excellent heat dissipating properties, the ability to provide a thin lubricant film, and its cleaning capacity to remove chips [22]. However, there is relatively limited literature accessible describing lubrication and cooling performance obtained with vegetable oil or ester-based water-soluble MWF in the machining of difficult-to-machine materials.

Most of these alternative lubrication/cooling systems on machining titanium alloys have been conducted on Ti6Al4V, so additional research is needed on other commercial and experimental alloys. There is little literature found on the work related to turning  $\gamma$ -TiAl. According to previous research achievements, when machining  $\gamma$ -TiAl alloy, the workpiece can suffer several surface damages and microstructural alterations, such as microcracks, redeposited materials, plastic deformation, cavities, and heat-affected zones [23]. Priarione et al. [24] studied the surface integrity and tool life when machining Ti-43.5Al-4Nb-1Mo-0.1B (TNM) with cubic boron nitride and polycrystalline diamond (PCD) coated inserts under conventional MWF cutting (6% emulsion) and cryogenic cooling with  $\text{LN}_2$ . Results showed that under cryogenic cooling, PCD tool life was increased compared to conventional MWF.

The significant influence of lubrication/cooling systems on the machinability of  $\gamma$ -TiAl alloys is shown by Kockle et al. [25]. The authors studied the effect of conventional MWF (6% mineral oil emulsion), MQL (vegetable oil with compressed air), dry, and  $\text{LN}_2$  cooling on the surface integrity and tool wear when turning Ti-45Al-2Nb-2Mn + 0.8 with uncoated cemented carbide tools. Results confirm that

dry condition is not appropriate for machining  $\gamma$ -TiAl. Compared to conventional MWF, with MQL, a slight decrease of the tool wear and a reduction of approximately 30% of surface roughness is achieved. However, the best results were obtained using cryogenic cooling.

To overcome these challenges of the machinability of  $\gamma$ -TiAl, this study responds to the need of replacing mineral-based MWF in turning  $\gamma$ -TiAl by introducing a formulation of a new sustainable ester-based water-soluble MWF (EcoMWF). It includes the evaluation of the performance obtained with an EcoMWF in comparison with conventional mineral oil-based water-soluble MWF and other green lubrication/cooling systems such as dry, CCA, MQL, and cryogenic; under different cutting parameters during finishing, repair, and/or maintenance turning processes in workpieces of the aeronautic industry. The effects of the lubrication/cooling systems, tool type (coated/uncoated carbide insert), and cutting parameters on the quality of the machined part (surface roughness and roundness), tool temperature, and tool wear have been studied with analysis of variance (ANOVA).

## 2 Experimental

### 2.1 Workpiece, Tools, and Equipment

A cylindrical bar of  $\gamma$ -TiAl was used to investigate the influence of lubrication/cooling systems and machining parameters on the horizontal turning, in particular, with a small depth of cut as the used in finishing, repair, and/or maintenance operations. The workpiece used was a Ti-43.5Al-4Nb-1Mo-0.1B alloy with 45 mm diameter and 250 mm in length. The turning tests were conducted on a parallel lathe (Pinacho model L-1/200). The selection of the cutting parameters for turning  $\gamma$ -TiAl is based on similar studies in the literature, referenced in Table 1.

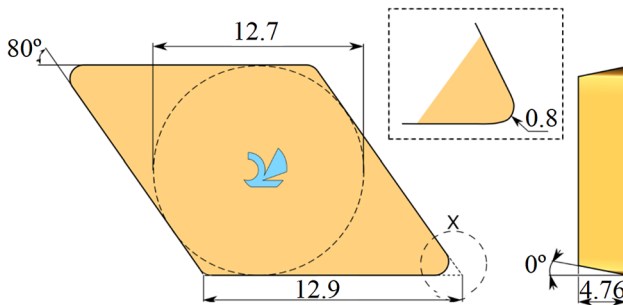
Spindle speed, feed rate, and insert type were selected as input machining parameters in different conditions of lubrication/cooling systems, while surface roughness, temperature, roundness, and tool wear were selected as response parameters. The experiments were carried out at two feed rates (0.14 and 0.28 mm/rev) and two spindle speeds (500 and 800 rpm), whereas the other two cutting parameters were kept constant (depth of cut = 0.03 mm and machining length = 120 mm). The tools used in the research were uncoated cemented carbide (883) and physical vapor deposition (PVD) coated carbide tools (TS2500) from Seco Tools (CNMG120408-M1-883 and CNMG120408-M1-TS2500 PVD manufacturer codes, respectively Fig. 2). A new insert cutting edge was used for each experimental run.

The influence of cutting parameters and different conditions of lubrication/cooling systems on the cutting

**Table 1** Cutting conditions for turning  $\gamma$ -TiAl alloy

References	Alloy	Machining parameters	Tool	Environment
Settineri et al. [26]	Ti-48Al-2Cr-2Nb, Ti-43.5Al-4Nb-1-Mo-0.1B, Ti-45Al-2Nb-2Mn+0.8	$v_c$ : 80 m/min; $a_p$ : 0.25 mm; $f$ : 0.1 mm	Uncoated cemented carbide	MWF
Kocke et al. [25]	Ti-45Al-2Nb-2Mn+0.8	$v_c$ : 80 m/min; $a_p$ : 0.25 mm; $f$ : 0.1 mm	Uncoated cemented carbide	MWF, cryogenic, dry, MQL
Cheng et al. [27]	Ti-47.5Al-2.5 V-1Cr	$v_c$ : 25–100 m/min; $a_p$ : 0.15–0.35 mm; $f$ : 0.05–0.2 mm/rev	Uncoated cemented carbide	MWF
Sharman et al. [23]	Ti-45Al-2Nb-2Mn+0.8	$v_c$ : 25–40 m/min; $a_p$ : 0.05–0.1 mm; $f$ : 0.05 mm/rev	Uncoated cemented carbide	MWF
Yao et al. [28]	$\gamma$ -TiAl	$v_c$ : 30–50 m/min; $a_p$ : 0.2–1 mm; $f$ : 0.06–0.1 mm/rev	PVD-coated carbide inserts	–
Priarone et al. [24]	Ti-43.5Al-4Nb-1Mo-0.1B	$v_c$ : 80 m/min; $a_p$ : 0.25 mm; $f$ : 0.1 mm	Cubic boron nitride and polycrystalline diamond (PCD)	MWF, cryogenic
Beranoagirre and López de la Calle [1]	Ti-44Al-6Nb-0.2C	$v_c$ : 40–60 m/min; $a_p$ : 0.5–2 mm; $f$ : 0.05–0.15 mm/rev	Tungsten carbide	MWF

$v_c$  cutting speed,  $a_p$  depth of cut,  $f$  feed

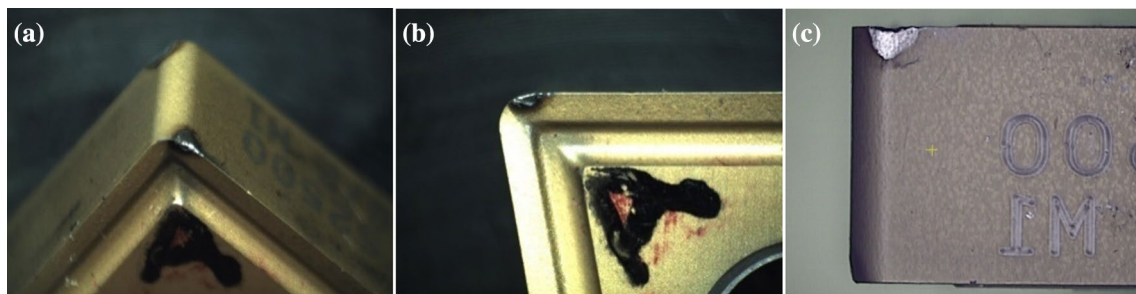
**Fig. 2** Geometry of the tested tools

temperature, surface quality, and tool were studied. Temperature at the tool interface was measured using an Optris CT model LT pyrometer, and the approximate cutting temperature was recorded. After the experiment, the surface

roughness of each cut was measured Mitutoyo SurfTest SJ 401 profilometer. The arithmetic averaged surface roughness ( $R_a$ ) was measured at 15 mm, 67 mm, and 110 mm.

The workpiece's roundness affects the dimension accuracy, the quality, and the suitability of the piece for assembly [29]. Roundness is the difference between the maximum and minimum radius. Based on the literature review, few studies report on the effect of cutting conditions on roundness in the turning of titanium alloys. In this study, the roundness was measured in the middle of the machined workpiece (60 mm) using Mitutoyo Roundtest RA-10.

The tool wear (Fig. 3) was analyzed using an optical microscope Euromex model ST, while the wear on the rake and flank faces of the inserts were measured using Tesa Visio DCC300. A detailed investigation of the worn tool to determine the main wear mechanisms during  $\gamma$ -TiAl turning under different lubrication/cooling systems was carried out

**Fig. 3** Microscopic image of TS2500 insert when machining at 0.14 mm/rev and 500 rpm: **a** tool wear, **b** rake, and **c** flank face

using Scanning Electron Microscope (SEM, model JEOL JSM-6010LV). Finally, the software of design of experiments was used to analyze the responses and determine the effect of the cutting parameters and the lubrication/cooling system, as well as the interactions among other factors.

## 2.2 Lubrication/Cooling Systems

The different cutting environments considered in this study include dry, cold-compressed air system (CCA), cryogenic, flood (12 l/min with EcoMWF and commercial MWF), and MQL (0.9 ml/min) (Fig. 4). For the CCA system, a Cold Air Gun Vortex system was used to achieve a cooling medium of  $-16.7^{\circ}\text{C}$ , measured at the injector exit point with Multi-metrix DMM220. In cryogenic cooling trials, liquid nitrogen has been conditioned in a 180-l ranger at low pressure, and an  $\text{LN}_2$  jet was applied on the insert.

EcoMWF for this study was formulated using a magnetic stirrer. A mixture of monoethanolamine (5.76 g), triethanolamine (5.64 g), and isononanoic acid (7.09 g) was added in deionized water and stirred for one hour. These raw materials have pH buffering capacity and are used to protect the workpiece and machine surface against corrosion. After, non-ionic surfactant (oleyl/cetyl propoxylated alcohol, 13.12 g) and anionic surfactant (oleth-10 carboxylic acid, 10.20 g) were used to reduce the surface tension of the fluid, to emulsify the ester in water, and to improve the lubricity of the cutting fluid [30]. A highly biodegradable trimethylolpropane trioleate ester (provided by Industrial Química Lasem, 6.44 g) and an eco-friendly phosphate ester (provided by Solvay, 12.14 g) were added to provide lubricity and anti-wear properties. Finally, 8.25 g of glycol was added to stabilize the mixture. The fluid was magnetically stirred at room temperature for two hours.

Before conducting experiments, the formulated EcoMWF and a commercial MWF (trade name Servol 634) containing mineral oil supplied by Brugarolas (Spain) were tested

in Labtap G8 (Microtap, Munich, Germany) with Ti6Al4V workpiece at 300 rpm spindle speed and 6 mm depth of cut. In the experiments, the MWFs were diluted at 10% in deionized water. Observing the results shown in Fig. 5, the tapping torque of the formulated MWF remains below the commercial. The increase in tapping torque is attributed to the increase in tool wear for each consecutive run. Therefore, the formulated EcoMWF was expected to provide better anti-wear performance than the commercial mineral-based lube in titanium alloys.

Chemically modified vegetable oils and fatty alcohols are the most common products for machining with the MQL system [31]. In this study, for the MQL environment, a trimethylolpropane trioleate was used as the same ester oil to formulate the EcoMWF. Figure 4b shows the MQL externally connected setup with a flow of 0.9 ml/min.

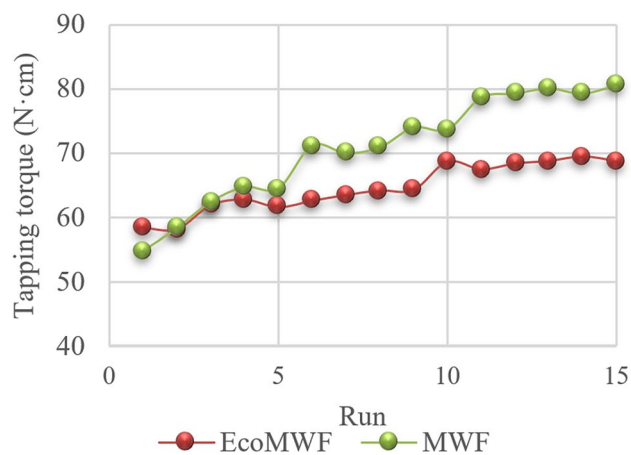
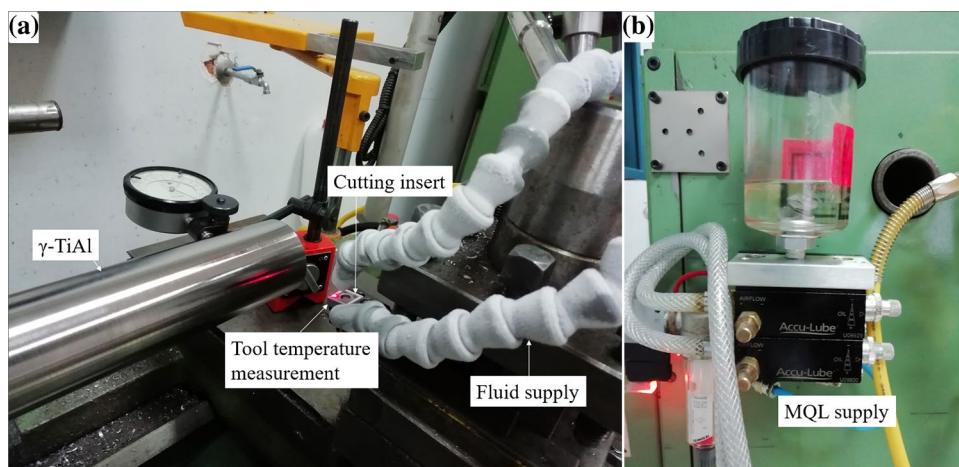


Fig. 5 Tapping torque results with machining consecutive taps with the formulated EcoMWF and commercial MWF

Fig. 4 Experimental configurations under different environments: **a** CCA, cryogenic and MWF fluid supply, and **b** MQL



### 3 Results

The objective of this work was to investigate the effects of input parameters on the surface roughness and the roundness of the  $\gamma$ -TiAl workpieces as well as the temperature at the tip of the tool, under different environments produced by dissimilar lubrication/cooling systems. The experimental data of the 2 (feed rate levels)  $\times$  2 (spindle speed levels)  $\times$  2 (insert type levels)  $\times$  6 (environment levels) = 48 cutting conditions are presented in the Appendix. Experimental data for the turning process of  $\gamma$ -TiAl.

Regarding the chips formed during machining, neither dry condition nor MQL systems could remove chips from the cutting zone, leading to an agglomeration of fine titanium chips that are highly combustible, and even in some experiments, sparks occurred. This danger is present with high cutting temperatures as the chips retain the heat and, worse yet, when oil-based lubricants are used in the machining [10]. Using water-based MWF eliminates the danger of ignition while it removes the chips. In the case of CCA and cryogenic cooling cutting, chips become brittle and easy to break. Furthermore, they offer the advantage that chips can be collected in dry and clean form.

#### 3.1 Tool Wear

Tool wear leads to decrease productivity while increasing machining costs. The inserts depicted in Figs. 6 and 7 show the microscopic images of the flank of the uncoated and PVD-coated insert, respectively, used in turning  $\gamma$ -TiAl at different cutting parameters with several lubrication/cooling systems. The examination of the inserts used for machining reveals that the lubrication/system and the insert type are the main parameters determining the tool life. Weather coated or uncoated, the cutting edge is characterized by clearly defined cracks.

At first glance, it is noticeable that the highest tool wear is achieved in dry conditions. Moreover, Fig. 8 shows the excessive wear on the rake face accompanied by discoloration of the uncoated carbide tool and temperature contours of the PVD tool due to the elevated temperatures associated with dry lubrication. The results confirm that dry machining is not appropriate for turning  $\gamma$ -TiAl due to the extreme tool wear.

Table 2 shows the results of the statistical analysis of the flank wear for the linear model. The model F-values of 6.25 implies that the model is significant. Spindle speed, insert type, and environment are significant model terms with p values below 0.0500.

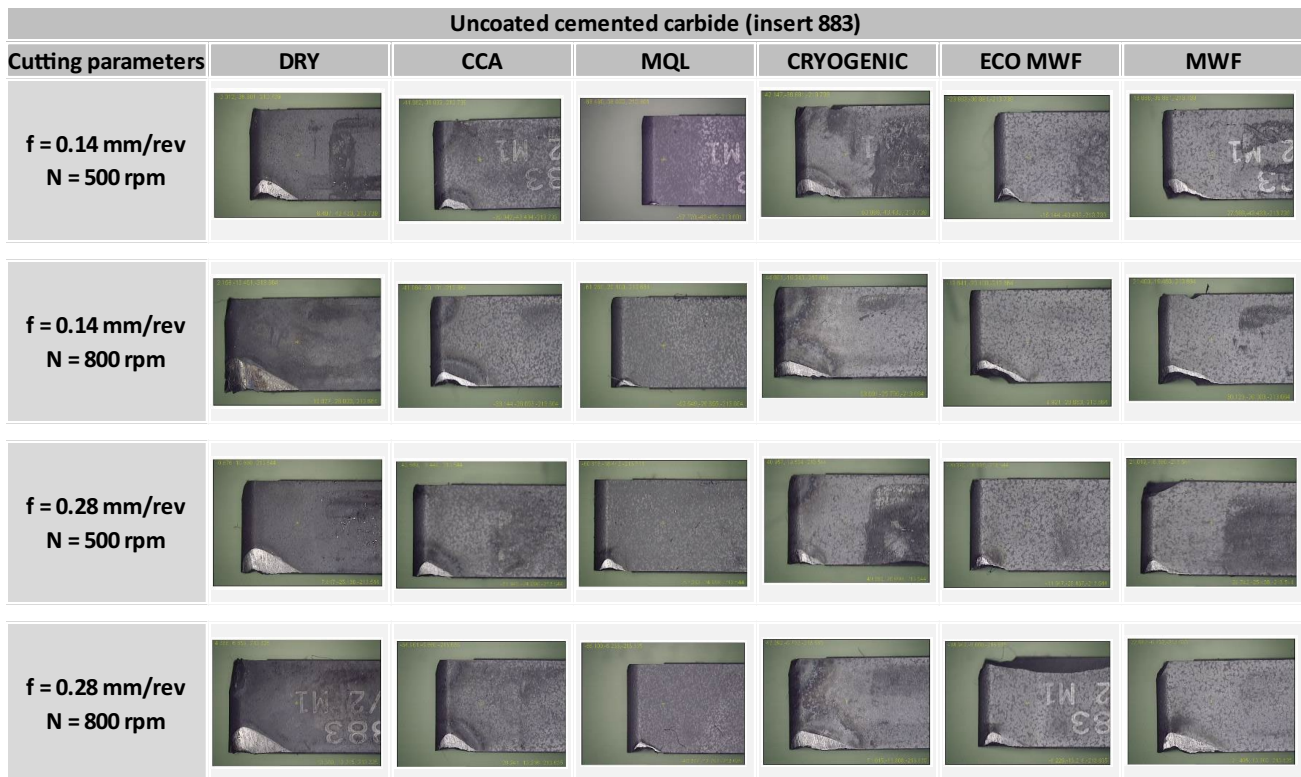


**Fig. 6** Microscopic images (objective  $\times 0.75$ ) of the flank of the uncoated insert used in turning  $\gamma$ -TiAl at different cutting parameters with different lubrication/cooling systems

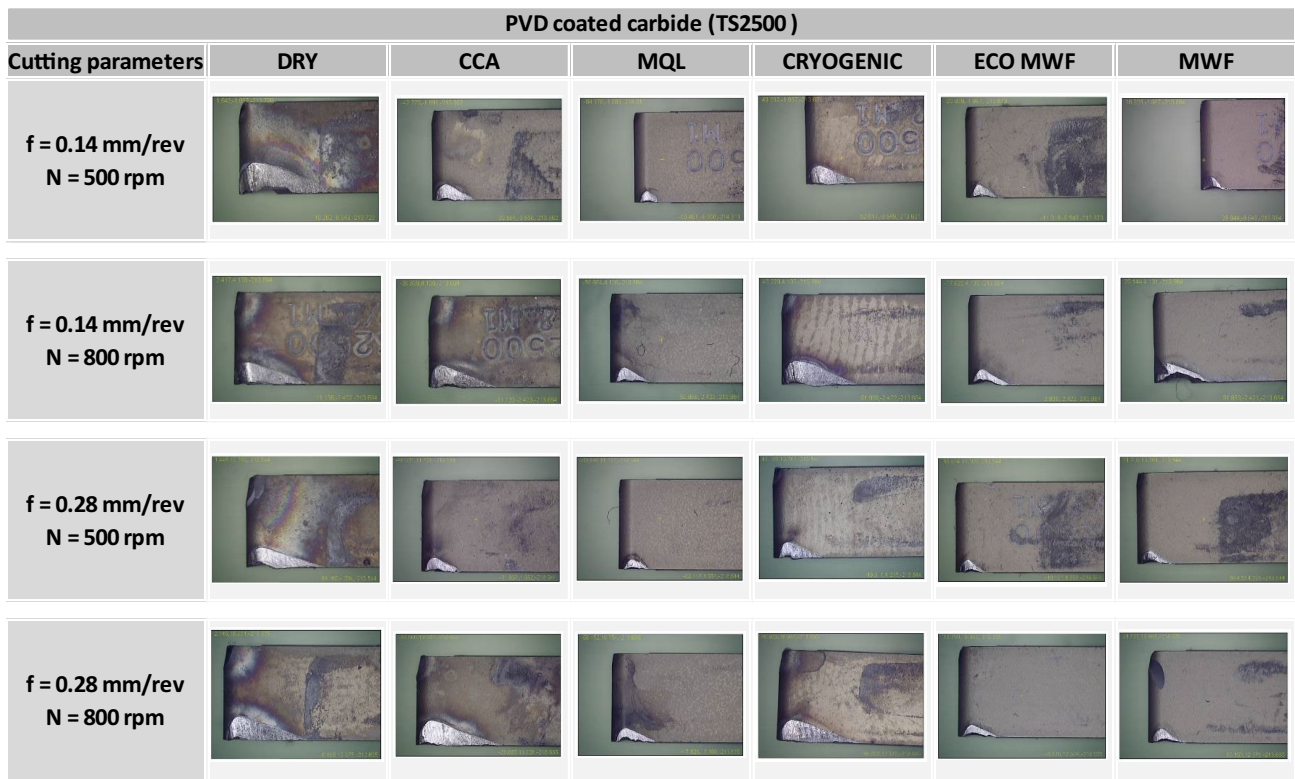


Fig. 7 Microscopic images (objective×0.75) of the flank of the PVD coated insert used in turning  $\gamma$ -TiAl at different cutting parameters with different lubrication/cooling systems

Fig. 8 Microscopic image of the insert during dry turning at 500 rpm and 0.28 mm/rev: **a** uncoated insert (883) and **b** with PVD coated insert (TS2500)

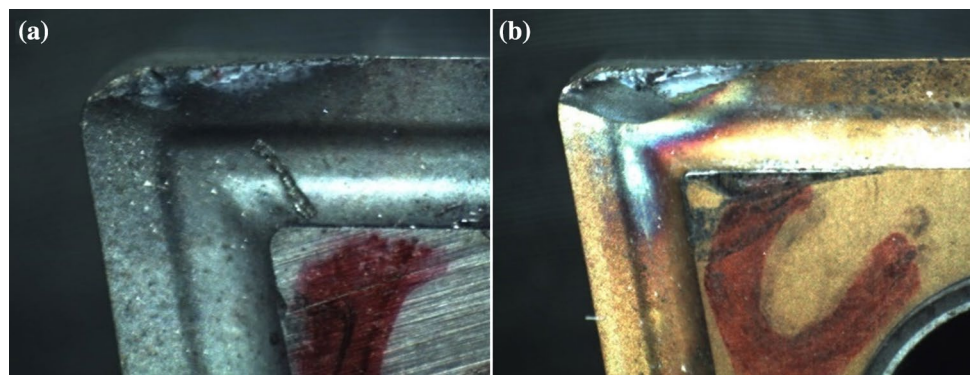


Table 2 Linear ANOVA model for flank wear after turning process

Source	Sum of squares	df	Mean square	F value	p value	
Model	4.12	8	0.5150	6.25	<0.0001	Significant
A-feed rate	0.1796	1	0.1796	2.18	0.1480	
<b>B-spindle speed</b>	0.9565	1	0.9565	<b>11.60</b>	0.0015	
<b>C-insert</b>	1.00	1	1.00	<b>12.14</b>	0.0012	
<b>D-environment</b>	1.98	5	0.3966	<b>4.81</b>	0.0016	
Residual	3.22	39	0.0824			
Cor total	7.33	47				

The most significant parameters and values in the model are highlighted in bold

Figure 9 shows the tool wear using two different tools. Each bar represents a different combination of feed rate and spindle speed, with bars grouped according to the lubrication/cooling system. The wear is more pronounced on the flank face rather than the rake face. The analysis shown in Fig. 9a indicates that the uncoated carbide inserts used during machining with MQL systems prolong the tool life. The high capability of the ester to form a lubricating film protects the surface from flank wear.

At low spindle speed (500 rpm), MQL, cryogenic, and EcoMWF are the lubrication/cooling systems that prevent further tool wear. Based on the experimental results, an increase in spindle speed tends to accelerate the flank wear. At these severe conditions, lubrication predominates over cooling capacity, with the lowest tool wear using MQL. The flank wear of uncoated carbide tools (883) is reduced using MQL. With this lubrication/cooling system, rake wear values of approximately 0.1 mm can be achieved.

The coating of the tool has a significant influence on its lifetime, especially in the case of flood systems, where the flank wear of the uncoated carbide tool is, in general, higher than PVD coated tool. The results indicate the benefits of MQL and flood systems in terms of tool life. At the lowest spindle speed of 500 rpm, the results for low (0.14 mm/

rev) and high (0.28 mm/rev) feed rates are nearly identical for MQL and flood systems. When turning  $\gamma$ -TiAl with EcoMWF, the TS2500 insert shows reduced flank and rake wear, especially for 500 rpm and 0.28 rev/min, where 0.5 mm<sup>2</sup> and 0.03 mm values are achieved, respectively. This emphasizes the effectiveness of liquid fluid in reducing the tool wear due to its lubrication film formation, which improves the tool performance and hence, productivity.

In addition to the quantification analysis of the tool wear, the type of wear was studied using SEM. Due to the relatively large number of variables considered in this research, the tools observed belong to a fixed cutting condition of spindle speed of 500 rpm and feed rate of 0.28 mm/rev. This was considered to be sufficient to study the impact of lubrication/cooling systems on tool wear. The wear on cutting tools occurred on the flank face and rake face, although significant wear was produced in the region of the tool nose when turning under dry, cryogenic, and CCA systems. A lack of lubrication effect causes an increase of tool nose wear due to higher friction at the tool-chip interface [32]. CCA shows similar wear characteristics as cryogenic system. It is also observed that between flood systems, EcoMWF and MWF, there are no significant changes in the wear type.

**Fig. 9** Tool wear at different cutting parameters with different lubrication/cooling systems: **a** flank wear area of uncoated insert (883), **b** rake wear of uncoated insert (883), **c** flank wear area of PVD coated insert (TS2500), and **d** rake wear of PVD coated insert (TS2500)

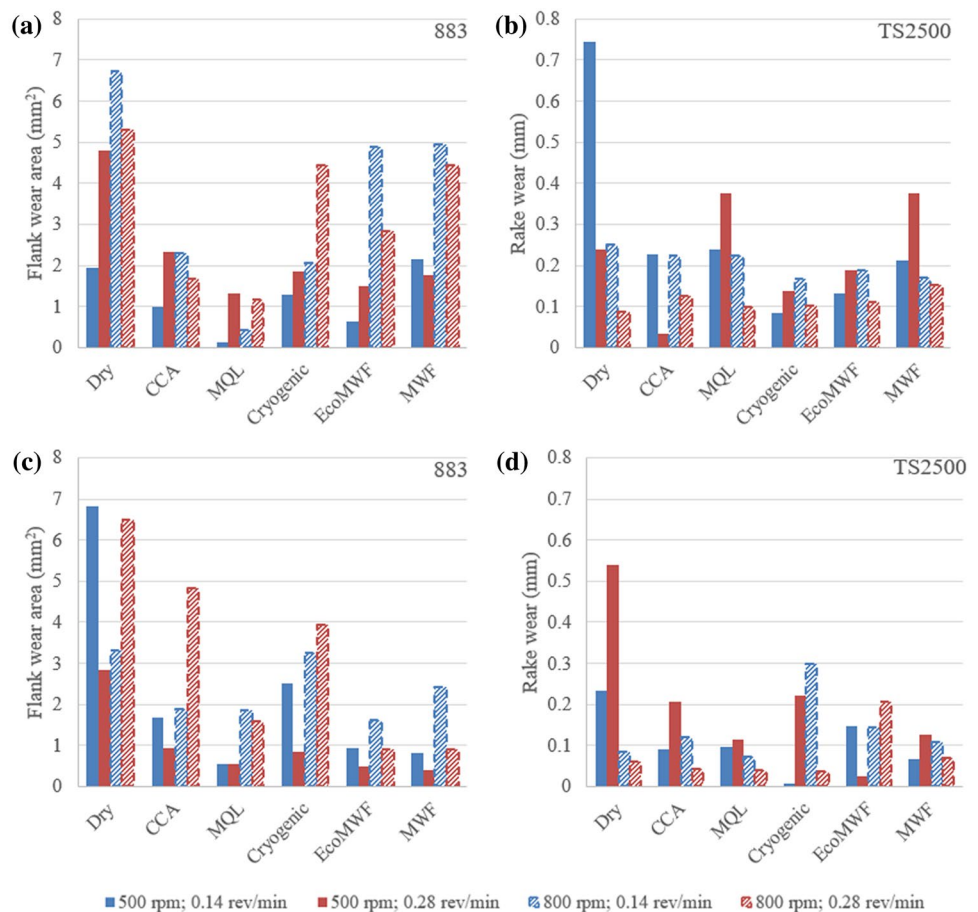




Figure 10 shows the wear types that occurred when turning  $\gamma$ -TiAl using uncoated carbide tools. The severity of tool wear caused catastrophic failure through edge fracture was noticed in all the tests. SEM observations of the damaged tools indicate that there is a high amount of adhered material onto the flank face. Compared to MQL, a smoother adherent layer is formed with flood systems.

Flank wear occurs on the flank face of the tool as a result of the friction between the newly cut surface of the workpiece and the tool flank. The wear initiates at the cutting edge and grows perpendicular to the flank face. Moreover, hard particles are observed on the flank face. These particles may originate from the tool either by the chip formation or the workpiece. The high temperature and the high pressure during machining cause the welding of these particles to the adherent layers of the flank face. Due to the problematic chip evacuation and low cooling effect of MQL, more hard particles weld to the cutting tool. During turning, chips rub in these adherent layers, yielding abrasive mechanisms. Abrasion could also have happened before adhesion, but, in most cases, it was not possible to observe it on the flank face.

From Fig. 11, the cutting edge crack is less for PVD coated carbide tools, although a high amount of adhered material is also observed in the flank face. Abrasive particles stick onto the tool surface and the adherent later. Examination of the worn coated tools revealed that the coating was removed from the substrate. Such delamination occurred with all lubrication/cooling systems used.

Adhesive wear takes place on both coating and substrate surfaces (Fig. 12). A possible explanation for this observable fact is that the workpiece material is adhered to the coating,

followed by flaking. As turning progresses, the material continues to adhere to the uncoated substrate. When the coating is removed, the worn tool presents similar wear behaviors to uncoated carbide tools.

A lost of material on the tool rake face and the formation of craters is observed in all cases. Crater wear is a common type of wear when turning titanium alloys, due to the chemical affinity between the workpiece and the cutting tool material [33]. Abrasive particles easily weld to the cutting edge and rake face leading through different wear types, especially with uncoated carbide tools. Figure 13 shows SEM images of uncoated and PVD coated tools after machining with MWF. Adhesion of workpiece material can be clearly seen on the worn area of the insert and that the coating has been flaking off.

### 3.2 Surface Roughness

The surface roughness of the workpiece was measured at 110, 67, and 15 mm ( $Ra_1$ ,  $Ra_2$ ,  $Ra_3$ , respectively). Figure 14 represents the surface roughness average obtained at different cutting parameters with coated and uncoated carbide tools for each length with each lubrication/cooling system. The surface roughness values obtained at the beginning of the turning operation ( $Ra_3$ ) are the highest. As the turning progresses, the surface roughness improves. In terms of workpiece quality, it is undesirable to obtain very different roughness along the workpiece length, which would require an additional finishing operation. When machining with the coated carbide tool, these increments are more prominent in the case of CCA, MQL, and MWF.

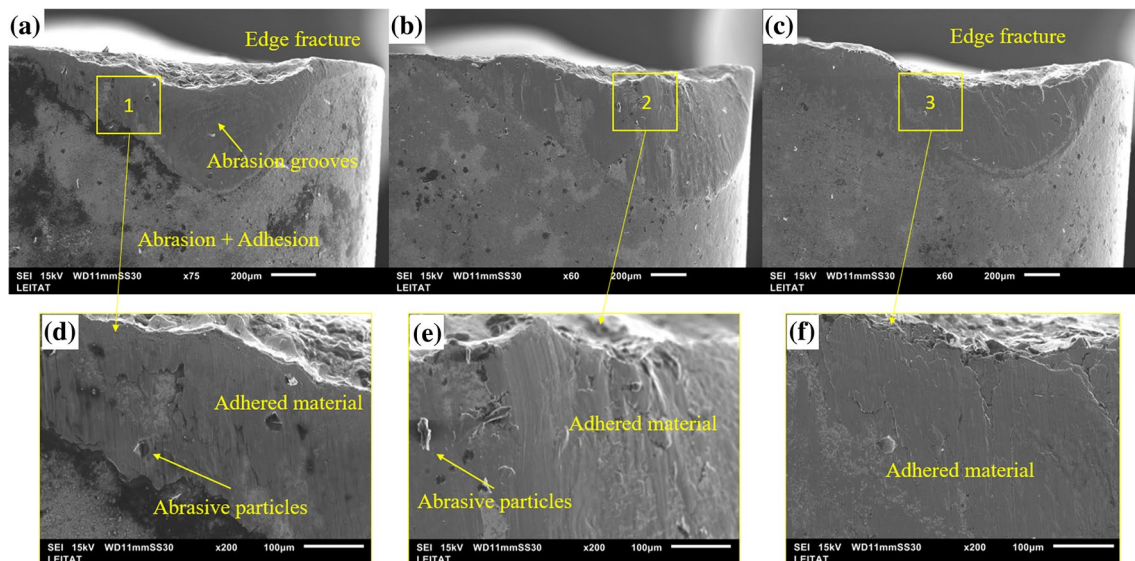


**Fig. 10** SEM images of the flank face uncoated carbide tool (883): **a** under MQL, **b** under cryogenic, **c** under MWF, **d** magnification of area 1, **e** magnification of area 2, and **f** magnification of area 3

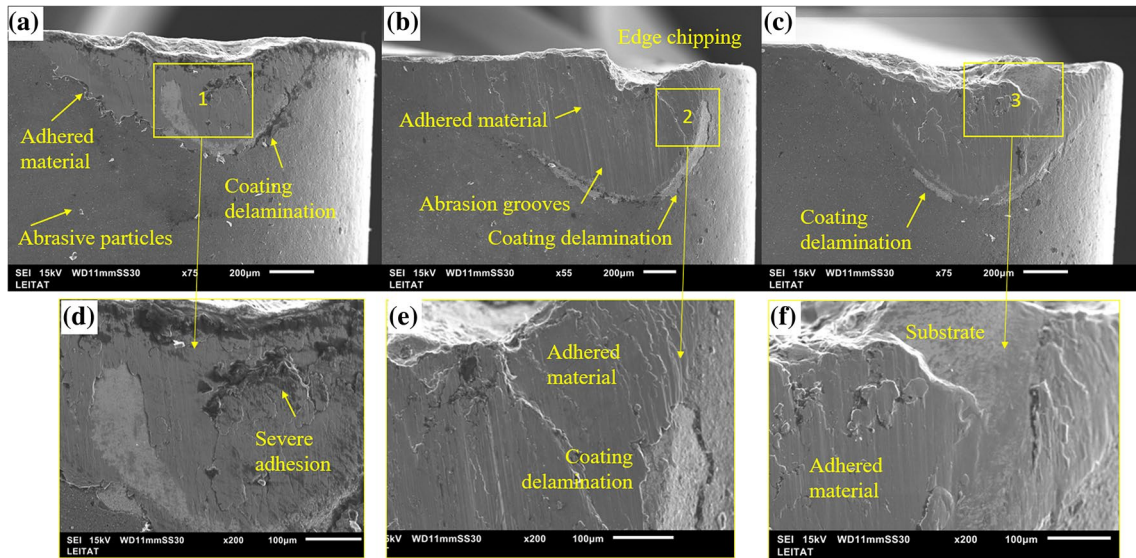


**Fig. 11** SEM images of the flank face coated carbide tool (TS2500): **a** under MQL, **b** under cryogenic, **c** under EcoMWF, **d** magnification of area 1, **e** magnification of area 2, and **f** magnification of area 3

**Fig. 12** Flank face areas of the PVD tool with adhered material: **a** on the coating and **b** on the substrate

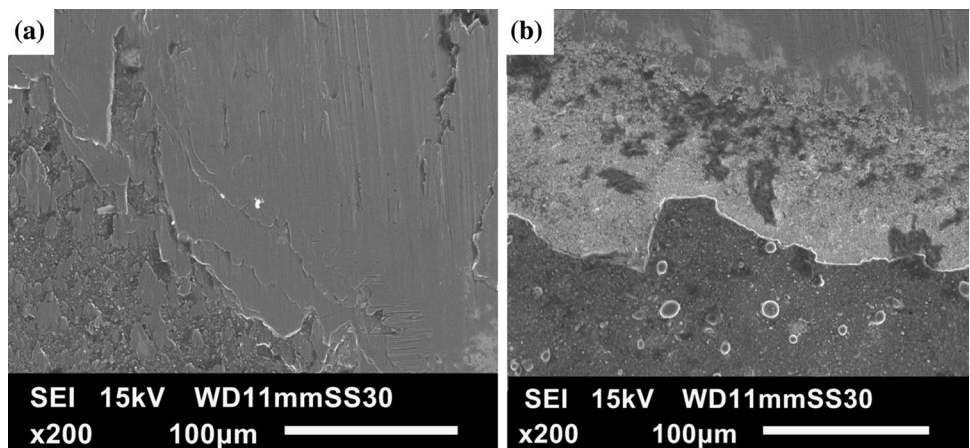
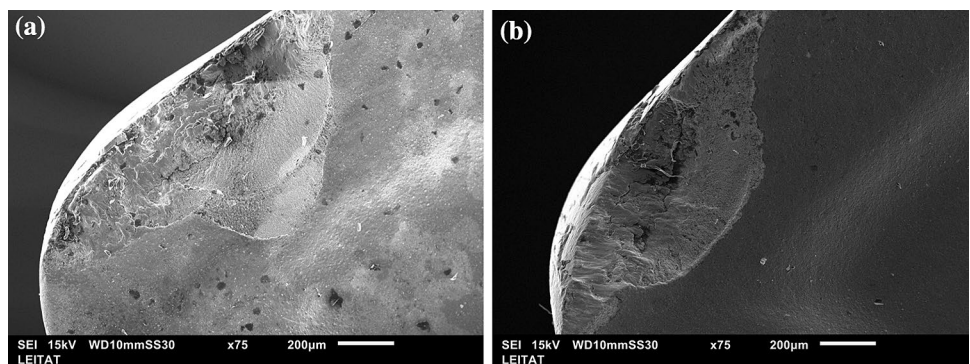


**Fig. 13** Rake face of the tool: **a** uncoated (883) and **b** PVD coated insert (TS2500)



The surface roughness average of  $Ra_1$ ,  $Ra_2$ , and  $Ra_3$  ( $Ra$ ) is used hereafter in the data post-analysis. The influence of varying the insert and environment on surface roughness

average at different machining parameters is shown Fig. 15. It can be observed that using EcoMWF, the surface roughness obtained is inside the aeronautic requirements (between

**Fig. 14** Surface roughness values measured at different lengths versus environment with **a** insert 883 and **b** insert TS2500

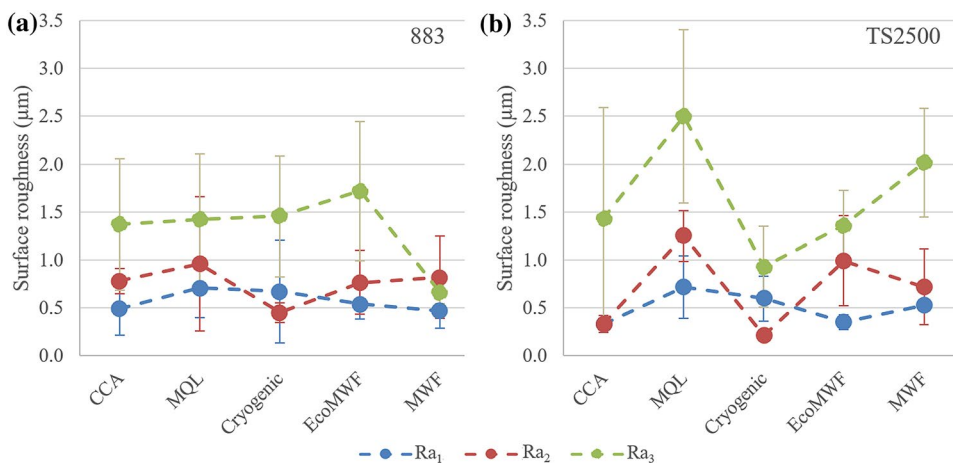
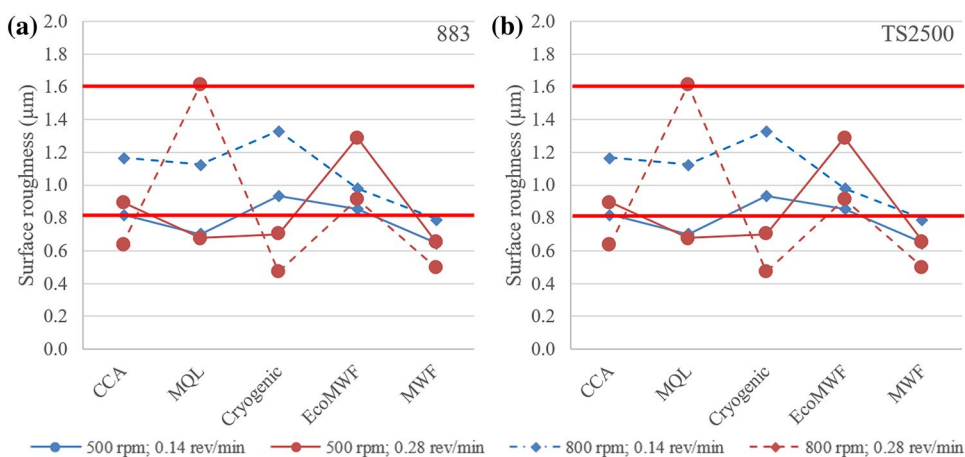


**Fig. 15** Surface roughness values, Ra, obtained at different cutting conditions for the different lubrication/cooling systems tested: **a** uncoated insert 883 and **b** coated insert TS2500. The red lines represent the range of the Ra values usually required in the aeronautic sector  $0.8 \text{ mm} < Ra < 1.6 \text{ mm}$



the range  $0.8 \text{ }\mu\text{m}$  to  $1.6 \text{ }\mu\text{m}$ ), according to the general criteria of the aeronautic industry [34]. In this case, only at the lowest cutting speed (500 rpm and  $0.14 \text{ mm/rev}$ ) with the coated tool, the surface roughness is slightly below the desired values.

In general, when machining at 800 rpm, the surface roughness values are lower by increasing the feed rate. Whereas, at 500 rpm, slight differences among results can be seen when varying feed rates. Surface roughness varies significantly over the lubrication/cooling system used during machining without any apparent relation to tool wear.

Main differences among lubrication/cooling systems are observed when machining with the uncoated carbide insert (883) at high cutting speed (800 rpm and  $0.28 \text{ mm/rev}$ ). Based on the results obtained,  $0.14 \text{ mm/rev}$  appears to be the optimum feed rate, where most of the surface roughness values are in the aeronautic requirements range. Compared to 883, after turning  $\gamma\text{-TiAl}$  with TS2500 insert, the lubrication/cooling systems influence is more significant. The use of MQL resulted in increased surface roughness.

### 3.3 Roundness

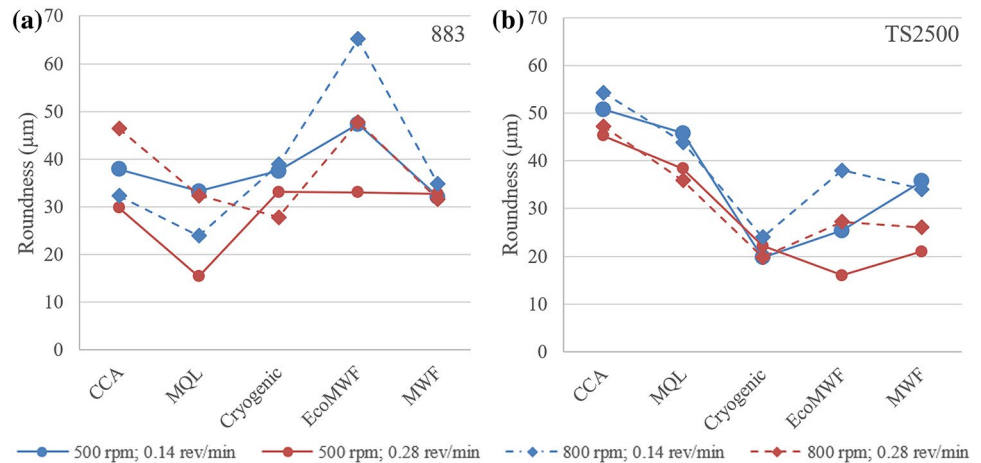
Roundness is a critical quality parameter during turning, influenced by radial force and elasticity of the material, and is indirectly associated with localized softening caused by localized heat generation [35]. Table 3 shows the ANOVA for the reduced two-factor model interaction (2FI) for roundness. An F value of 10.35 implies that the model is significant. In this case, the feed rate, the environment, and its relationship with the insert type are the most significant model terms.

Figure 16 presents the influence of using various lubrication/cooling systems on roundness. By analyzing the results for roundness, different trends to those in surface roughness can be observed. When turning  $\gamma\text{-TiAl}$  with the uncoated carbide inserts (883), the roundness of the workpiece tends to vary depending on the machining parameters. The PVD-coated tool (TS2500) achieved the best results, and they also show a workpiece quality increase by increasing the feed rate. By comparing flood systems, roundness values do not

**Table 3** Reduced 2FI ANOVA model for roundness after turning operation

Source	Sum of squares	df	Mean square	F value	p value	
Model	4811.65	18	267.31	10.35	<0.0001	Significant
<b>A-feed rate</b>	368.02	1	368.02	<b>14.25</b>	0.0007	
B-spindle speed	125.68	1	125.68	4.87	0.0355	
C-insert	3.09	1	3.09	0.1195	0.7321	
<b>D-environment</b>	1830.86	5	366.17	<b>14.18</b>	<0.0001	
BD	310.47	5	62.09	2.40	0.0610	
<b>CD</b>	2173.53	5	434.71	<b>16.83</b>	<0.0001	
Residual	748.93	29	25.83			
Cor Total	5560.58	47				

The most significant parameters and values in the model are highlighted in bold

**Fig. 16** Influence of insert and environment on the roundness: **a** insert 883 and **b** insert TS2500

show significant changes between the commercial mineral-based MWF and the EcoMWF.

### 3.4 Temperature

The temperature of the cutting tool depends on the heat generated during turning and the ability of the lubrication/cooling system to dissipate heat. Figure 17 shows the cutting temperatures measured for each lubricating and machining condition. The bar chart indicates the increasing temperature during the turning process, with a maximum temperature of 654 °C in dry machining and a minimum of 11 °C with the cryogenic system. As feed rate and spindle speed increase, machining times are reduced (shortened bars).

The temperature sensor cannot measure in MWF environment conditions due to the liquid blocks the measurement. However, the heat-affected zone on the coated tool and the white interface layer on the carbide tool, generated due to heat accumulation, is shown in dry, MQL, and CCA systems, but not on cryogenic and flood systems. The high-water content in EcoMWF and MWF allows removing heat from the machining operation, thus reducing the temperature.

The results of ANOVA for the linear model (Table 4) show the strong influence of the environment on the maximum temperature. The cryogenic system shows the lowest cutting temperatures measured. LN<sub>2</sub> absorbs the heat generated during the metal cutting and evaporates rapidly. In this media, the machining conditions where the tool temperature achieves the highest values (348 °C) is at 0.14 mm/rev, 800 rpm, and using the PVD coated insert.

The temperature of the tool, under CCA and MQL conditions, stood at the lowest compared to dry ones. In dry conditions, the absence of fluid neither lubricates nor removes heat from the cutting zone, increasing the temperature during turning and achieving maximum values of 654 °C at 500 rpm and 0.28 mm/rev with the PVD coated insert. Compared to cryogenic, the MQL system has a reduced cooling capacity due to the low amount of fluid that reached the cutting zone and the low thermal conductivity of ester compared to water, causing the temperature to increase substantially.

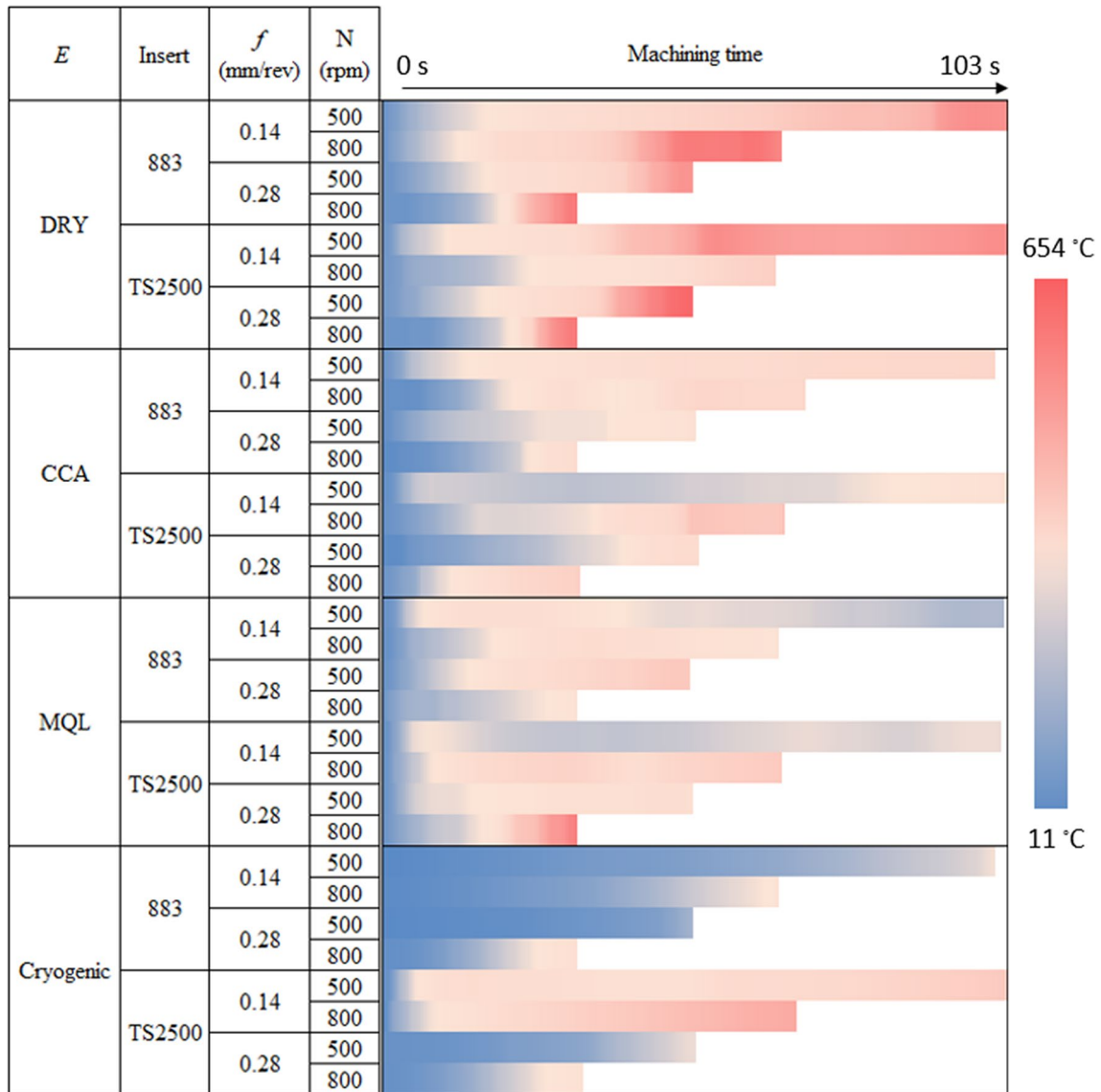


Fig. 17 Influence of the lubrication/cooling system, tool, and machining parameters on the temperature of the tool

Table 4 Linear ANOVA model for maximum temperature achieved during the turning operation

Source	Sum of squares	ff	Mean square	F value	p value	
Model	12.02	6	2.00	7.42	0.0001	Significant
A-feed rate	0.0097	1	0.0097	0.0358	0.8514	
B-spindle speed	0.5507	1	0.5507	2.04	0.1655	
C-insert	0.4911	1	0.4911	1.82	0.1894	
<b>D-environment</b>	10.97	3	3.66	<b>13.55</b>	<0.0001	
Residual	6.75	25	0.2698			
Cor Total	18.76	31				

The most significant parameters and values in the model are highlighted in bold

## 4 Discussion

From the results shown above, the lubrication/cooling system used on the machinability of gamma titanium aluminides alloy has shown a high impact on tool wear, surface roughness, and roundness. The wear types usually observed when machining titanium aluminides include flank wear, crater wear, chipping, and fracture of the cutting edge [4]. The cutting tool presents different wear mechanisms depending on the tool areas. SEM observations indicate that the predominant tool wear mechanism is adhesion, followed by attrition of workpiece material on the flank and rake surface, which cause severe tool wear. Under all cutting conditions, the removal of tool material by the adherent material (attrition) was observed on the cutting edge.

In most cases, the adhered layer was found mainly on the flank face rather than on the rake face. This suggests that the adhered material on the rake face had been removed, causing chipping of tool material. As wear increases, the tool is subjected to more force and heat, leading to a higher temperature in the cutting zone and higher vibrations. Many sparks are produced when flood systems are not used. Coated carbide tools show a low beneficial impact on the tool's wear due to the severe crater wear that rapidly removes the coating, leading to an exposed substrate. However, the coating delays various wear types and helps increase tool life.

There is no clear relationship between surface roughness and tool wear. This performance can be explained, in part, by the increased edge radius, which can improve surface roughness [36]. According to the study of Derani and Ratnam [37], a decrease in  $R_a$  is often interpreted as an improvement in surface roughness. However, as the authors explained,  $R_a$  can decrease due to gradual tool wear. During finish turning, the nose region of the tool engages the workpiece and shapes the surface profile. The theoretical surface roughness can be estimated by the following equation [9]:

$$R_a = 0.032 \frac{f^2}{r} \quad (1)$$

where  $f$  is the feed rate and  $r$  is the tool nose radius.

There are two main reasons why surface roughness varies during machining for a fixed feed rate. On one hand, the wear, chipping, or fracture at the nose region, changes the effective nose radius. On the other hand, the increase of the tool wear flank causes tool chatter and vibration that affects the surface quality of the workpiece [37]. During machining, the surface roughness values decreased. Initially, when the tool is new and, the nose radius is 0.8 mm,  $R_a$  values are close to the theoretical  $R_a$ . As cutting progresses, the insert tends to suffer excessive nose wear. The nose radius increases, and following Eq. 1,  $R_a$  decreases.

This also explains why the surface roughness values using cryogenic and CCA systems are lower than MQL and flood systems, especially when machining with the coated carbide tool. It is observed from Fig. 18 that the nose region of the tool is seriously damaged under cryogenic machining, those reducing the effective nose radius. However, it cannot be dismissed that other types of tool wear, the temperature on the cutting zone, chip flushing capability, and vibration, can affect the surface roughness of the workpiece. For instance, due to the lack of chip evacuation of MQL systems and the low plasticity of  $\gamma$ -TiAl alloy, the chip can scratch the workpiece surface, leading to an increase of  $R_a$  values [28].

Considering both tool wear and surface roughness, when turning with TS2500 tool, EcoMWF offered the best performance at 500 rpm and 0.28 rev/min. With 883 tool, the best alternative is the use of MQL at 800 rpm and 0.28 rev/min, flowed by CCA and EcoMWF at 500 rpm and 0.14 rev/min. The absence of lubrication and cooling functions during dry machining leads to higher friction and higher cutting temperature, which results in severe tool wear and catastrophic failure. Under flood machining, metalworking fluids reduce the heat generated and remove abrasive particles from the cutting zone. Moreover, metalworking fluids form an organic

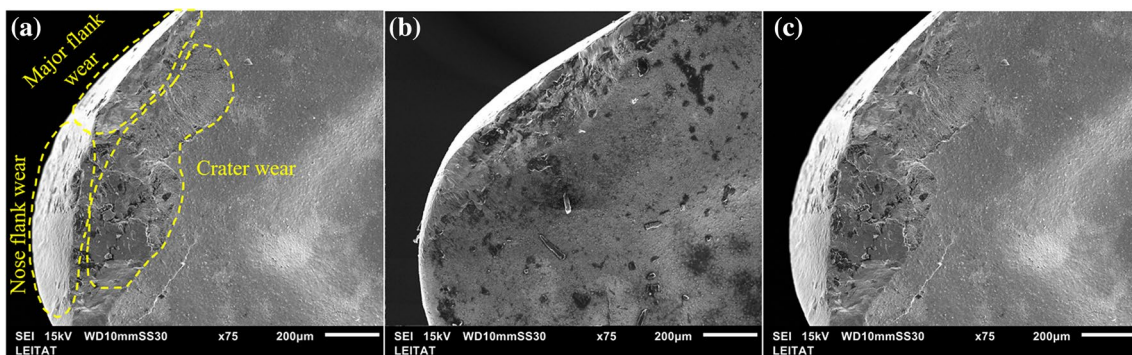


**Fig. 18** SEM images of tool rake face when turning  $\gamma$ -TiAl with uncoated carbide tool at 500 rpm and 0.28 mm/rev: **a** tool wear types, **b** under MQL and **c** under cryogenic

film on the metal surface, thus reducing the cutting forces and tool wear [38]. Comparing the two metalworking fluids, EcoMWF showed lower tapping torque values than conventional MWF (Fig. 4). When using MWF, the rapid tool wear increases the cutting forces measured during tapping, which is highly sensitive to lubrication [39].

During finish turning with MQL, an ester is supplied in the cutting zone. The ester adheres to the surface, forming a lubricant film, which reduces friction forces and tool wear. The high viscosity of the ester, compared to metalworking fluids, tends to resist the flow, thus providing a more effective lubricating at the tool-chip interface, which reduces friction and prevents rapid tool wear [40]. However, the poor chip evacuation and low cooling capacity cause higher surface roughness values.

On the contrary, the use of LN<sub>2</sub> and CCA improves the effective cooling action due to the extremely low temperatures. The fluid supply pressure removes the abrasive particles, although it is less efficient than flood systems. Compared to MQL, when turning with cryogenic and CCA systems, the flank wear increases, particularly with PVD coated carbide tools. This may be attributed to the lack of lubrication and the abrasive mechanism, which leads to flank and nose wear. The coating of the insert is removed and followed by an abrasion of the base tool material and adhesion of workpiece.

The evaluation of the eco-efficiency of the lubrication/cooling systems considers the technical and environmental impacts for each lubrication/cooling system. Additionally, some features should be considered, as the ability to remove chips, fire prevention, and its economic and environmental aspects. All the features of the generated data are rescaled within the range of 1 (worst) to 5 (best). All the indices in the radar chart (Fig. 19) have been considered of equal importance. From Fig. 19, the eco-efficiency of each lubrication/cooling system can be easily established.

Eliminating the lubrication/cooling system, as in dry machining, has shown a reduced capacity to remove heat from the cutting zone, resulting excessive tool wear and

catastrophic tool failure. Moreover, its low chip evacuation causes fire due to the agglomeration of metal particles and the high temperature in the cutting zone. In addition, although it is advantageous in terms of environmental impact because there is no fluid consumption and no fluid residue on the workpiece or chips to be treated, there is a high cost of tools due to their short life. Therefore, this analysis confirms that dry machining is not suited for turning  $\gamma$ -TiAl.

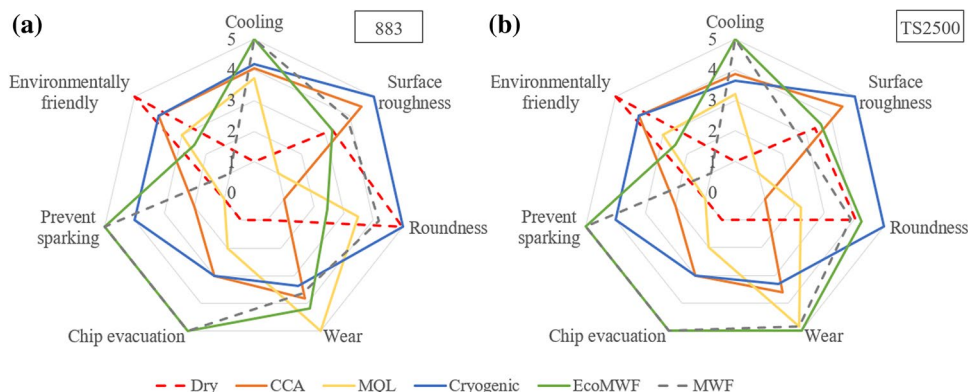
The application of cold-compressed air in turning  $\gamma$ -TiAl improves the cooling capacity, but not enough to avoid spark. Additionally, in terms of roundness and surface roughness, the workpiece quality is highly dependent on the cutting speed. CCA is considered one of the cleanest lubrication/cooling systems.

Using cryogenic not only can reduce tool temperature but also enhance the workpiece quality. LN<sub>2</sub> absorbs the heat generated during cutting and evaporates without leaving a harmful residue. However, its reduced lubricating capacity results in excessive tool wear, regardless of the tool used. Despite the high electrical energy consumption to produce LN<sub>2</sub> [41], it is an alternative that may be of particular interest in special operations.

To make a remarkable reduction in the MWF consumption, MQL was studied. Due to its high affinity with the surface, it forms a lubricating film resulting in a reduction of tool wear. The biodegradable ester used as a lubricating fluid is consumed entirely during the turning operation, eliminating the need for fluid disposal. Nevertheless, like dry machining, there is a problematic chip evacuation which, together with the organic ester, increases the probability of fire hazard.

Flood system can effectively remove heat and chips from the cutting zone, resulting in longer tool life and prevents sparking. The use of EcoMWF and MWF resulted in reduced surface roughness. Using EcoMWF, surface roughness values are within the parameters of the aeronautic industry ( $0.8 \text{ mm} < Ra < 1.6 \text{ mm}$ ). The presence of the tool coating appears to have a beneficial effect on tool wear and surface quality. Comparing the two flood systems, EcoMWF

**Fig. 19** Radar chart with the general perspective of the technical and environmental impact for each lubrication/cooling system with **a** uncoated carbide tool (883) and **b** PVD coated carbide tool (TS2500)



formulation leads to reduced tool wear, enhancing the use of this system as an alternative to mineral-based MWF. Moreover, the properties of EcoMWF based on esters reduce the contribution to global warming compared to fossil carbon sources by nearly four times [42].

## 5 Conclusions

This work compares different sustainable lubrication/cooling systems that can be employed in repair and maintenance turning operations of aeronautic industry workpieces made of  $\gamma$ -TiAl. In particular, the feasibility of using the EcoMWF developed ad hoc for this study. Tool wear, surface roughness (in terms of Ra), roundness and cutting temperature have been analyzed as response variables. Following are the main conclusion drawn from this study:

- From the observations using SEM on the worn tools, it can be concluded that the tools failed primarily on the flank and rake faces of the insert. Crater, nose wear, and adhesion of material were observed. The underlying wear mechanisms responsible for these types of wear were characterized mainly as abrasive and adhesive, giving rise to attrition. Furthermore, due to the removal of the coating material, TS2500 fails similar to the uncoated tool 883.
- Tool wear could be a key performance indicator to compare different lubrication/cooling systems, while surface roughness data could lead to incorrect conclusions if other changes on the profile topography are ignored. Further work should include the study of the subsurface deformation and microstructure alteration of the workpiece.
- The PVD-coated tool also shows promising results in the machinability of  $\gamma$ -TiAl. After turning  $\gamma$ -TiAl with TS2500 insert, flank wear is significantly lower than with the uncoated carbide tool (883), especially under MQL and flood systems.
- The statistical analysis showed that the lubrication/cooling system is the most influential parameter in the turning process of  $\gamma$ -TiAl. Also, the interaction of environment and tool types has a significant influence on surface roughness and roundness.
- At all the cutting speeds, MQL has outperformed in terms of tool wear (flank and rake) compared to dry, cryogenic, and CCA machining conditions. Hence, flood systems (EcoMWF and MWF) performed the best machining for the turning of  $\gamma$ -TiAl within the selected range of cutting parameters and the TS2500 tool.
- Considering both tool wear and surface roughness, when turning with TS2500 tool, EcoMWF offered the best performance at 500 rpm and 0.28 rev/min. With 883 tool, the best alternative is the use of MQL at 800 rpm and 0.28 rev/min, flowed by CCA and EcoMWF at 500 rpm and 0.14 rev/min.
- Overall, the formulated water-based MWF with a synthetic ester (EcoMWF) can be identified as a lubrication/cooling system to potentially enhance cutting performance through tool wear reduction and surface quality enhancement, as at the same time the environmental and health are reduced.

The novelty of this work depends upon exploring some green lubrication/cooling systems to improve the machinability of third-generation  $\gamma$ -TiAl and the formulation of a newly eco-efficient water-based MWF. Future research may focus on the machinability of hybrid lubricating/cooling systems such as MQL together with cold-compressed air or cryogenic cooling for gamma titanium aluminides.



## Appendix: Experimental Data for the Turning Process of $\gamma$ -TiAl

Run	Insert	$f$ (mm/rev)	$N$ (rpm)	Environment	Ra at 110 mm $Ra_1$ ( $\mu\text{m}$ )	Ra at 67 mm $Ra_2$ ( $\mu\text{m}$ )	Ra at 15 mm $Ra_3$ ( $\mu\text{m}$ )	Roundness ( $\mu\text{m}$ )	Temperature ( $^{\circ}\text{C}$ )
1	883	0.14	500	MQL	0.64	0.64	0.82	33.26	108.1
2	883	0.14	800	MQL	0.61	0.50	2.27	23.96	115.6
3	883	0.28	500	MQL	0.43	0.70	0.90	15.44	206.2
4	883	0.28	800	MQL	1.15	2.00	1.69	32.37	88.7
5	TS2500	0.14	500	MQL	1.18	1.50	1.53	45.81	74.5
6	TS2500	0.14	800	MQL	0.41	1.39	3.66	43.89	195.7
7	TS2500	0.28	500	MQL	0.63	1.22	2.70	38.42	105.8
8	TS2500	0.28	800	MQL	0.66	0.89	2.11	35.89	533.4
9	883	0.14	500	DRY	0.29	1.18	1.20	19.17	480.1
10	883	0.14	800	DRY	0.47	0.19	2.71	18.77	598.5
11	883	0.28	500	DRY	0.42	0.34	1.86	20.64	452.9
12	883	0.28	800	DRY	0.66	0.56	1.54	22.81	566.2
13	883	0.14	500	CCA	0.49	0.77	1.20	37.92	145.3
14	883	0.14	800	CCA	0.26	0.86	2.38	32.30	145.5
15	883	0.28	500	CCA	0.87	0.89	0.93	29.80	98.8
16	883	0.28	800	CCA	0.33	0.60	0.97	46.40	116.2
17	TS2500	0.14	500	DRY	0.52	0.39	0.42	29.79	487.4
18	TS2500	0.14	800	DRY	0.64	0.27	0.57	32.59	173.0
19	TS2500	0.28	500	DRY	0.35	0.22	0.89	27.67	654.0
20	TS2500	0.28	800	DRY	0.46	0.33	0.43	21.83	565.2
21	TS2500	0.14	500	CCA	0.28	0.40	0.48	50.80	104.3
22	TS2500	0.14	800	CCA	0.34	0.20	3.03	54.26	231.8
23	TS2500	0.28	500	CCA	0.33	0.36	1.54	45.27	115.3
24	TS2500	0.28	800	CCA	0.37	0.36	0.66	47.22	166.1
25	883	0.14	500	Cryogenic	0.34	0.55	1.91	37.50	73.4
26	883	0.14	800	Cryogenic	1.47	0.48	2.04	38.93	81.3
27	883	0.28	500	Cryogenic	0.46	0.46	1.18	33.10	40.6
28	883	0.28	800	Cryogenic	0.41	0.31	0.70	27.84	101.5
29	TS2500	0.14	500	Cryogenic	0.29	0.23	0.68	19.71	205.7
30	TS2500	0.14	800	Cryogenic	0.72	0.17	1.28	23.98	347.9
31	TS2500	0.28	500	Cryogenic	0.83	0.22	1.29	22.20	69.4
32	TS2500	0.28	800	Cryogenic	0.55	0.23	0.46	19.82	89.8
33	883	0.14	500	EcoMWF	0.48	1.25	0.83	47.31	-
34	883	0.14	800	EcoMWF	0.35	0.54	2.05	65.20	-
35	883	0.28	500	EcoMWF	0.64	0.72	2.51	33.08	-
36	883	0.28	800	EcoMWF	0.70	0.55	1.49	47.79	-
37	TS2500	0.14	500	EcoMWF	0.33	0.57	0.84	25.42	-
38	TS2500	0.14	800	EcoMWF	0.27	1.17	1.43	38.00	-
39	TS2500	0.28	500	EcoMWF	0.45	0.65	1.47	16.03	-
40	TS2500	0.28	800	EcoMWF	0.35	1.57	1.70	27.25	-
41	883	0.14	500	MWF	0.72	0.61	0.61	32.11	-
42	883	0.14	800	MWF	0.43	1.36	0.59	34.78	-
43	883	0.28	500	MWF	0.42	0.94	0.61	32.74	-
44	883	0.28	800	MWF	0.30	0.37	0.83	31.61	-
45	TS2500	0.14	500	MWF	0.46	0.46	2.83	35.70	-
46	TS2500	0.14	800	MWF	0.57	0.74	1.70	34.04	-

Run	Insert	$f$ (mm/rev)	$N$ (rpm)	Environment	Ra at 110 mm $Ra_1$ ( $\mu\text{m}$ )	Ra at 67 mm $Ra_2$ ( $\mu\text{m}$ )	Ra at 15 mm $Ra_3$ ( $\mu\text{m}$ )	Roundness ( $\mu\text{m}$ )	Temperature (°C)
47	TS2500	0.28	500	MWF	0.55	0.41	1.57	21.02	-
48	TS2500	0.28	800	MWF	0.54	1.27	1.96	26.05	-

**Acknowledgements** The authors thank the UNED funding for open access publishing and the Research Group of the UNED “Industrial Production and Manufacturing Engineering (IPME)” for the support given during the development of this work, which has been financed in part by the Spanish Ministry of Science, Innovation and Universities (Project RTI2018-102215-B-I00), to the Industrial Engineering School-UNED (REF2022-ICF04), and to the Master in Advanced Manufacturing Engineering.

**Author Contributions** EB conceptualization, methodology, validation, formal analysis, investigation, resources, data curation, writing—original draft preparation, writing—review and editing. EMR conceptualization, methodology, validation, formal analysis, writing—review and editing, supervision, project administration, funding acquisition. LA conceptualization, formal analysis, writing—review and editing. MAS-N formal analysis.

**Funding** Open Access funding provided thanks to the CRUE-CSIC agreement with Springer Nature.

## Declarations

**Conflict of interest** The authors declare that they have no known competing financial interests or personal relationships that could have appeared to influence the work reported in this paper.

**Open Access** This article is licensed under a Creative Commons Attribution 4.0 International License, which permits use, sharing, adaptation, distribution and reproduction in any medium or format, as long as you give appropriate credit to the original author(s) and the source, provide a link to the Creative Commons licence, and indicate if changes were made. The images or other third party material in this article are included in the article's Creative Commons licence, unless indicated otherwise in a credit line to the material. If material is not included in the article's Creative Commons licence and your intended use is not permitted by statutory regulation or exceeds the permitted use, you will need to obtain permission directly from the copyright holder. To view a copy of this licence, visit <http://creativecommons.org/licenses/by/4.0/>.

## References

- Beranoagirre, A., & López De Lacalle, L. N. (2012). Turning of gamma TiAl intermetallic alloys. *AIP Conference Proceedings*, 1431, 526–532. <https://doi.org/10.1063/1.4707605>
- Clemens, H., & Kestler, H. (2000). Processing and applications of intermetallic  $\gamma$ -TiAl-based alloys. *Advanced Engineering Materials*, 2, 551–570. [https://doi.org/10.1002/1527-2648\(200009\)2:9%3c551::AID-ADEM551%3e3.0.CO;2-U](https://doi.org/10.1002/1527-2648(200009)2:9%3c551::AID-ADEM551%3e3.0.CO;2-U)
- Clemens, H., & Mayer, S. (2016). Intermetallic titanium aluminides in aerospace applications—Processing, microstructure and properties. *Materials at High Temperatures*, 33, 560–570. <https://doi.org/10.1080/09603409.2016.1163792>
- Aspinwall, D. K., Dewes, R. C., & Mantle, A. L. (2005). The machining of  $\gamma$ -TiAl intermetallic alloys. *CIRP Annals—Manufacturing Technology*, 54, 99–104. [https://doi.org/10.1016/S0007-8506\(07\)60059-6](https://doi.org/10.1016/S0007-8506(07)60059-6)
- Oke, S. R., Ogunwande, G. S., Onifade, M., Aikulola, E., Adewale, E. D., Olawale, O. E., Ayodele, B. E., Mwema, F., Obiko, J., & Bodunrin, M. O. (2020). An overview of conventional and non-conventional techniques for machining of titanium alloys. *Manufacturing Review*. <https://doi.org/10.1051/mfreview/2020029>
- Dahar, M. S., Tamirisakandala, S. A., & Lewandowski, J. J. (2018). Evolution of fatigue crack growth and fracture behavior in gamma titanium aluminide Ti-43.5Al-4Nb-1Mo-0.1B (TNM) forgings. *International Journal of Fatigue*, 111, 54–69. <https://doi.org/10.1016/j.ijfatigue.2018.01.026>
- Schwaighofer, E., Rashkova, B., Clemens, H., Stark, A., & Mayer, S. (2014). Effect of carbon addition on solidification behavior, phase evolution and creep properties of an intermetallic  $\beta$ -stabilized  $\gamma$ -TiAl based alloy. *Intermetallics*, 46, 173–184. <https://doi.org/10.1016/j.intermet.2013.11.011>
- Schwaighofer, E., Clemens, H., Mayer, S., Lindemann, J., Klose, J., Smarsly, W., & Güther, V. (2014). Microstructural design and mechanical properties of a cast and heat-treated intermetallic multi-phase  $\gamma$ -TiAl based alloy. *Intermetallics*, 44, 128–140. <https://doi.org/10.1016/j.intermet.2013.09.010>
- Brinksmeier, E., Meyer, D., Huesmann-Cordes, A., & Herrmann, C. (2015). Metalworking fluids - Mechanisms and performance. *CIRP Annals—Manufacturing Technology*, 64, 605–628. <https://doi.org/10.1016/j.cirp.2015.05.003>
- Abdalla, H. S., Baines, W., McIntyre, G., & Slade, C. (2007). Development of novel sustainable neat-oil metal working fluids for stainless steel and titanium alloy machining. Part I. Formulation development. *The International Journal of Advanced Manufacturing Technology*, 34, 21–33. <https://doi.org/10.1007/s00170-006-0585-4>
- Gupta, M. K., Song, Q., Liu, Z., Sarikaya, M., Jamil, M., Mia, M., Kushvaha, V., Singla, A. K., & Li, Z. (2020). Ecological, economical and technological perspectives based sustainability assessment in hybrid-cooling assisted machining of Ti-6Al-4V alloy. *Sustainable Materials and Technologies*, 26, e00218. <https://doi.org/10.1016/j.susmat.2020.e00218>
- Wickramasinghe, K. C., Sasahara, H., Rahim, E. A., & Perera, G. I. P. (2020). Green metalworking fluids for sustainable machining applications: A review. *Journal of Cleaner Production*, 257, 120552. <https://doi.org/10.1016/j.jclepro.2020.120552>
- Benedicto, E., Carou, D., & Rubio, E. M. (2017). Technical, economic and environmental review of the lubrication/cooling systems used in machining processes. *Procedia Engineering*, 184, 99–116. <https://doi.org/10.1016/j.proeng.2017.04.075>
- Nouari, M., & Makich, H. (2013). Experimental investigation on the effect of the material microstructure on tool wear when machining hard titanium alloys: Ti-6Al-4V and Ti-555. *The International Journal of Refractory Metals and Hard Materials*, 41, 259–269. <https://doi.org/10.1016/j.ijrmhm.2013.04.011>
- Gaurav, G., Sharma, A., Dangayach, G. S., & Meena, M. L. (2020). Assessment of jojoba as a pure and nano-fluid base oil in minimum quantity lubrication (MQL) hard-turning of Ti-6Al-4V: A step towards sustainable machining. *Journal of Cleaner Production*, 272, 122553. <https://doi.org/10.1016/j.jclepro.2020.122553>

16. Klocke, F., Sangermann, H., Krämer, A., & Lung, D. (2011). Influence of a high-pressure lubricoolant supply on thermo-mechanical tool load and tool wear behaviour in the turning of aerospace materials. *The Proceedings of the Institution of Mechanical Engineers, Part B: Journal of Engineering Manufacture*, 225, 52–61. <https://doi.org/10.1177/09544054JEM2082>
17. Elshwain, A., Redzuan, N., Yusof, N. M., & Engineering, M. (2013). Machinability of nickel and titanium alloys under of gas-based coolant-lubricants (CLs)—A review. *International Journal of Research in Engineering and Technology*, 2, 690–702. <https://doi.org/10.15623/ijret.2013.0211106>
18. Shokrani, A., Dhokia, V., & Newman, S. (2012). Environmentally conscious machining of difficult-to-machine materials with regard to cutting fluids. *International Journal of Machine Tools and Manufacture*, 57, 83–101. <https://doi.org/10.1016/j.ijmactools.2012.02.002>
19. Agrawal, C., Wadhwa, J., Pitroda, A., Pruncu, C. I., Sarikaya, M., & Khanna, N. (2021). Comprehensive analysis of tool wear, tool life, surface roughness, costing and carbon emissions in turning Ti–6Al–4V titanium alloy: Cryogenic versus wet machining. *Tribology International*, 153, 106597. <https://doi.org/10.1016/j.triboint.2020.106597>
20. Nazma Sultana, M., Ranjan Dhar, N., & Binte Zaman, P. (2019). A review on different cooling/lubrication techniques in metal cutting. *American Journal of Mechanics and Applications*, 7, 71. <https://doi.org/10.11648/j.ajma.20190704.11>
21. Chetan, Ghosh, S., & Venkateswara-Rao, P. (2015). Application of sustainable techniques in metal cutting for enhanced machinability: A review. *Journal of Cleaner Production*, 100, 17–34. <https://doi.org/10.1016/j.jclepro.2015.03.039>
22. Yang, Y., Zhang, C., Wang, Y., Dai, Y., & Luo, J. (2016). Friction and wear performance of titanium alloy against tungsten carbide lubricated with phosphate ester. *Tribology International*, 95, 27–34. <https://doi.org/10.1016/j.triboint.2015.10.031>
23. Sharman, A. R. C., Aspinwall, D. K., Dewes, R. C., & Bowen, P. (2001). Workpiece surface integrity considerations when finish turning gamma titanium aluminide. *Wear*, 249, 473–481. [https://doi.org/10.1016/S0043-1648\(01\)00575-0](https://doi.org/10.1016/S0043-1648(01)00575-0)
24. Priarone, P. C., Klocke, F., Faga, M. G., Lung, D., & Settineri, L. (2016). Tool life and surface integrity when turning titanium aluminides with PCD tools under conventional wet cutting and cryogenic cooling. *International Journal of Advanced Manufacturing Technology*, 85, 807–816. <https://doi.org/10.1007/s00170-015-7958-5>
25. Klocke, F., Settineri, L., Lung, D., Claudio Priarone, P., & Arft, M. (2013). High performance cutting of gamma titanium aluminides: Influence of lubricoolant strategy on tool wear and surface integrity. *Wear*, 302, 1136–1144. <https://doi.org/10.1016/j.wear.2012.12.035>
26. Settineri, L., Priarone, P. C., Arft, M., Lung, D., & Stoyanov, T. (2014). An evaluative approach to correlate machinability, microstructures, and material properties of gamma titanium aluminides. *CIRP Annals—Manufacturing Technology*, 63, 57–60. <https://doi.org/10.1016/j.cirp.2014.03.068>
27. Cheng, Y., Yuan, Q., Zhang, B., & Wang, Z. (2019). Study on turning force of  $\gamma$ -TiAl alloy. *International Journal of Advanced Manufacturing Technology*, 105, 2393–2402. <https://doi.org/10.1007/s00170-019-04356-z>
28. Yao, C., Lin, J., Wu, D., & Ren, J. (2018). Surface integrity and fatigue behavior when turning  $\gamma$ -TiAl alloy with optimized PVD-coated carbide inserts. *Chinese Journal of Aeronautics*, 31, 826–836. <https://doi.org/10.1016/j.cja.2017.06.002>
29. Du, C. L., Luo, C. X., Han, Z. T., & Zhu, Y. S. (2014). Applying particle swarm optimization algorithm to roundness error evaluation based on minimum zone circle. *Measurement: Journal of the International Measurement Confederation*, 52, 12–21. <https://doi.org/10.1016/j.measurement.2014.02.028>
30. Benedicto, E., Rubio, E. M., Carou, D., & Santacruz, C. (2020). The role of surfactant structure on the development of a sustainable and effective cutting fluid for machining titanium alloys. *Metals (Basel)*, 10, 1388. <https://doi.org/10.3390/met10101388>
31. Weinert, K., Inasaki, I., Sutherland, J. W., & Wakabayashi, T. (2004). Dry machining and minimum quantity lubrication. *CIRP Annals—Manufacturing Technology*, 53, 511–537. [https://doi.org/10.1016/S0007-8506\(07\)60027-4](https://doi.org/10.1016/S0007-8506(07)60027-4)
32. Nath, C., Kapoor, S. G., Srivastava, A. K., & Iverson, J. (2013). Effect of fluid concentration in titanium machining with an atomization-based cutting fluid (ACF) spray system. *Journal of Manufacturing Processes*, 15, 419–425. <https://doi.org/10.1016/j.jmapro.2013.06.002>
33. Sartori, S., Taccin, M., Pavese, G., Ghiotti, A., & Bruschi, S. (2017). Wear mechanisms of uncoated and coated carbide tools when machining Ti6Al4V using LN2 and cooled N2. *The International Journal of Advanced Manufacturing Technology*. <https://doi.org/10.1007/s00170-017-1289-7>
34. Blanco, D., Rubio, E. M., Marín, M. M., & Davim, J. P. (2020). Repairing hybrid Mg–Al–Mg components using sustainable cooling systems. *Materials (Basel)*, 13, 393. <https://doi.org/10.3390/ma13020393>
35. Pramanik, A., & Littlefair, G. (2015). Machining of titanium alloy (Ti-6Al-4V)—Theory to application. *Machining Science and Technology*, 19, 1–49. <https://doi.org/10.1080/10910344.2014.991031>
36. Castellanos, S. D., Cavaleiro, A. J., Jesus, A. M. P. D., Neto, R., & Alves, J. L. (2019). Machinability of titanium aluminides: A review. *Proceedings of the Institution of Mechanical Engineers Part L Journal of Materials Design and Applications*, 233, 426–451. <https://doi.org/10.1177/1464420718809386>
37. Derani, M. N., & Ratnam, M. M. (2021). The use of tool flank wear and average roughness in assessing effectiveness of vegetable oils as cutting fluids during turning—A critical review. *International Journal of Advanced Manufacturing Technology*, 112, 1841–1871. <https://doi.org/10.1007/s00170-020-06490-5>
38. Benedicto, E., Rubio, E. M., Aubouy, L., & Sáenz-Nuño, M. A. (2021). Formulation of sustainable water-based cutting fluids with polyol esters for machining titanium alloys. *Metals (Basel)*, 11, 773. <https://doi.org/10.3390/met11050773>
39. Pereira, I. C., Da Silva, M. B., Da Cunha, D. F., & Sales, W. F. (2016). Analysis of tapping process in three types of cast iron. *International Journal of Advanced Manufacturing Technology*, 82, 1041–1048. <https://doi.org/10.1007/s00170-015-7430-6>
40. Rahim, E. A., & Sasahara, H. (2011). A study of the effect of palm oil as MQL lubricant on high speed drilling of titanium alloys. *Tribology International*, 44, 309–317. <https://doi.org/10.1016/j.triboint.2010.10.032>
41. Pušavec, F., & Kopač, J. (2011). Sustainability assessment: Cryogenic machining of Inconel 718. *Strojniški Vestnik Journal of Mechanical Engineering*, 57, 637–647. <https://doi.org/10.5545/sv-jme.2010.249>
42. Ekman, A., & Börjesson, P. (2011). Life cycle assessment of mineral oil-based and vegetable oil-based hydraulic fluids including comparison of biocatalytic and conventional production methods. *International Journal of Life Cycle Assessment*, 16, 297–305. <https://doi.org/10.1007/s11367-011-0263-0>

**Publisher's Note** Springer Nature remains neutral with regard to jurisdictional claims in published maps and institutional affiliations.



**Elisabet Benedicto** is a Chemical Engineer and Industrial Engineer from Institut Químic de Sarrià (IQS). She made a Master's in Advanced Manufacturing Engineering at UNED (National Distance Education University), where is doing a Ph.D. in Industrial Technologies focused on sustainable lubrication/cooling systems for titanium machining. In 2011 she joined LEITAT Technology Center, working on homecare products development. Today, she develops her professional career in the business unit

of Applied Chemistry and Materials as a principal investigator in the area of Surface Chemistry. She is specialized in the research and development of projects in the field of industrial fluids, focused on the formulation of lubricants and industrial detergents.



**Eva María Rubio** is Aeronautical Engineer (1997) from the Polytechnic University of Madrid and PhD in Industrial Engineering (2002) from the National University of Distance Education (UNED). Currently, she is a Full Professor at UNED, in the Manufacturing Engineering Department of the School of Industrial Engineering. Her main research interests include the following research areas: analysis of machining processes, analysis of metalforming processes, additive manufacturing, industrial

metrology, and teaching and innovation in engineering.



**Laurent Aubouy** is an Engineer in Material Sciences from de the ENSI-CAEN, Ph.D in Organic Chemistry from the University of Montpellier and MBA from EUNCET Business School with more than 20 years of experience in Applied Research and Development.



**María Ana Sáenz-Nuño** assistant professor in the Institute for Research in Technology at Comillas Universidad Pontificia since 2000. Before, she was a researcher in the National Metrology Institute in Spain, the Centro Español de Metrología (CEM) for almost 7 years and nowadays an active collaborator in most of its areas. She has supervised a Ph. D. in airturbines, has several scientific papers on metrology matters related with different fields and participated in many congresses

and workshops. She has been since 1998 member of the Spanish standardization committee on Metrology, working closely with the ISO/TC 213 and participate in the most important Spanish committees involved with metrology. Her research area is on Metrology and uncertainty in high resolution measurements, Health Metrology and Bioengineering.

## Authors and Affiliations

Elisabet Benedicto<sup>1,2,4</sup>  · Eva María Rubio<sup>1</sup> · Laurent Aubouy<sup>2</sup> · María Ana Sáenz-Nuño<sup>3</sup> 

<sup>1</sup> Department of Manufacturing Engineering, Universidad Nacional de Educación a Distancia (UNED), C/Juan del Rosal 12, 28040 Madrid, Spain

<sup>2</sup> Department of Surface Chemistry, Leitiat Technological Center, C/Innovació, 2, 08225 Terrassa, Spain

<sup>3</sup> Department of Manufacturing Engineering, Comillas Pontifical University, St/Alberto Aguilera 25, 28015 Madrid, Spain

<sup>4</sup> Programa de Doctorado en Tecnologías Industriales, Madrid, Spain